Imaging of amyloid-β deposits in brains of living mice permits direct observation of clearance of plaques with immunotherapy

BRIAN J. BACSKAI[1], STEPHEN T. KAJDASZ[1], RICHARD H. CHRISTIE[1], CORDELIA CARTER[1], DORA GAMES[2], PETER SEUBERT[2], DALE SCHENK[2] & BRADLEY T. HYMAN[1]

[1]*Alzheimer's Disease Research Laboratory, Massachusetts General Hospital, Charlestown, Massachusetts, USA*

[2]*Elan Pharmaceuticals, South San Francisco, California, USA*

Correspondence should be addressed to B.H.; email: b_hyman@helix.mgh.harvard.edu

Alzheimer disease (AD) can be diagnosed with certainty only post-mortem, by histologically demonstrating insoluble aggregates of amyloid-β peptide, called senile plaques[1–4]. Direct imaging of these lesions in the living brain would revolutionize early diagnosis of AD. Such imaging would also provide a powerful approach to monitor effects of putative anti-amyloid-β agents. However, the plaques are far too small to detect by conventional imaging techniques. The goal of this study was to develop novel imaging approaches, using *in vivo* multiphoton microscopy, to image senile plaques in PDAPP transgenic mice, which express a mutant human amyloid-β precursor protein and accumulate amyloid-β deposits[5,6]. We developed two robust methods: *in vivo* histology using the fluorescent histochemical dye thioflavine S, and *in vivo* immunofluorescence using labeled antibodies specific for amyloid-β. Immunization with amyloid-β peptide has been shown to prevent plaques in PDAPP mice[7]. We used our imaging techniques to test the hypothesis that existing plaques can be cleared by immunotherapy.

Multiphoton microscopy in the live mouse

Multiphoton microscopy uses relatively benign, long-wavelength light to excite standard fluorophores[8,9]. An advantage of multiphoton microscopy is that excitation occurs only in the focal volume of the objective lens that focuses the laser[8]. By contrast, in conventional confocal microscopy, the entire depth of tissue is exposed to potentially damaging high-energy light and only a small portion of the resulting fluorescence contributes to the image. Optical imaging permits a resolution on the order of one micron, two orders of magnitude higher than conventional *in vivo* imaging techniques, such as positron-emission topography or magnetic-resonance imaging[10]. With multiphoton microscopy, tightly focused images of microscopic structures or lesions can be obtained several hundred micrometers below the surface of the brain in a live animal.

In vivo imaging of senile plaques

Thioflavine S is a standard fluorescent stain that specifically binds to amyloid protein deposits; it is commonly used in neuropathological studies of AD. We applied a dilute solution of thioflavine S (which fluoresces in the blue–green range) to the cortical surface of a living mouse. After 20 minutes, we obtained a stack of optical thin sections in 2-μm steps. We observed dense-cored thioflavine S-positive plaques and amyloid angiopathy up to 150 μm deep to the surface of the brain, into layers II and III of the mouse cortex (Fig. 1*a* and *d*). We also developed a method for imaging amyloid-β deposits with *in vivo* immunofluorescence. A monoclonal antibody specific for amyloid-β, 10D5 (ref. 11), was labeled with fluorescein and applied directly to the cortex. Imaging of the cortex in a living 20-month-old PDAPP mouse revealed numerous amyloid-β deposits, some of which had characteristics of diffuse amyloid and others of which had discrete cores (Fig. 1*b* and *d*). The diffuse deposits had a fine morphology with frequent extensions, irregular shapes and clusters identical to the image observed by conventional histological immunostaining. Amyloid angiopathy on vessels of the pia mater was stained with thioflavine S and antibodies against amyloid-β (Fig. 1*d*). Thus, fluorescently labeled anti-amyloid-β antibodies diffused into the cortex and specifically labeled amyloid-β deposits, allowing imaging by multiphoton microscopy. Simultaneous injection of Texas Red-labeled dextran into a tail vein allowed visualization of capillaries and larger vessels, providing a 'road map' for re-imaging (Fig. 1*c* and *d*). Thus, the combined techniques demonstrate simultaneous *in vivo* histology, immunofluorescence and angiography (Fig. 1*d*).

Clearance of amyloid-β deposits by immunotherapy

As innumerable senile plaques are already present in the cortex of patients with dementia, therapeutic strategies must not only decrease new amyloid-β production and deposition, but they must reverse deposits that already exist. Our current experiments were prompted by the observation that immunization of PDAPP mice with amyloid-β leads to the prevention of new amyloid-β deposits[7]. We tested whether *in vivo* interaction of an anti-amyloid-β antibody with a plaque would lead to its clearance. We imaged amyloid-β deposits using thioflavine S in living mice before and after therapeutic intervention (Fig. 2). Mice were anesthetized, and a 1–1.5-mm craniotomy was performed. Thioflavine S and a solution of antibody (~1 mg/ml, 8 μl) was applied to the cranial window. The animal was imaged and allowed to recover. Three days later the animal was re-anesthetized and the same volume was imaged. Texas-Red angiography and stage location assured that the exact same volume was being imaged. Mice (n = 9) were randomly assigned to groups treated with either 10D5 or 16B5 (the latter is a monoclonal antibody directed against an intracellular epitope of human tau, which does not cross react with rodent tau[12]). Two blinded readers scored the presence of thioflavine-S plaques in each of 28 stacks of images (representing over 1,200 individual 1,024 × 1,024 pixel images), and compared first and second imaging sets to determine whether individual thioflavine-S plaques had been cleared. In the 10D5 group,

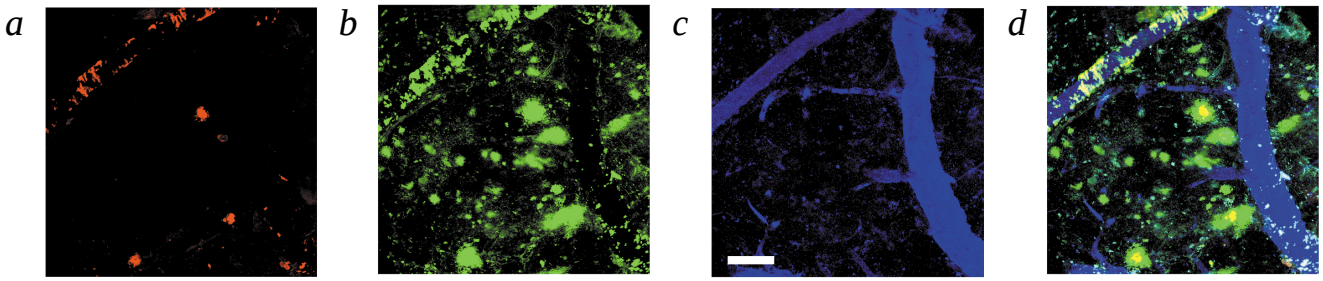

Fig. 1 Imaging of amyloid-β deposits in the live mouse. Thioflavine S, a fluorescent probe that binds to dense-core amyloid-β deposits, and fluorescein-labeled anti-amyloid-β antibody (10D5) were applied for 20 min directly to the surface of the brain of a living, anesthetized, 20-month-old homozygote PDAPP mouse. A solution of Texas Red-dextran (70,000 MW, Molecular Probes) was injected in a tail vein. Multiphoton microscopy permitted simultaneous 3-color fluorescence detection. Three-dimensional reconstructions of the images (Voxblast, VayTek, Fairfield, Iowa) on a Windows-NT based workstation (Precision 610, Dell Computer, Round Rock, Texas) are presented here. ***a***, Thioflavine-S localization shown in red with 4 dense-core plaques in this field, as well as amyloid angiopathy on the blood vessel in the top left corner. ***b***, *In vivo* immunofluorescence with labeled anti-amyloid-β antibodies, which stain both fibrillar and diffuse amyloid-β deposits (green). ***c***, Fluorescent angiography (blue) provides 3-D fiduciary points to allow lining up imaging volumes within the same animal over time. ***d***, Merged panels (*a*–*c*) into one 24-bit image, where the thioflavine S-positive plaques and amyloid angiopathy are seen as yellow, surrounded by difuse amyloid-β deposits in green. Scale bar, 100 μm.

45 of 65 plaques (70%) were cleared 3 days after initial imaging. In the 16B5 group, only 9 of 45 plaques were cleared after 3 days (20%; $\chi^2 = 30.5$, $P < 0.001$).

This result demonstrates that dense-core amyloid-β deposits are reversed by 10D5 application. We next examined whether all immunodetectable forms of amyloid-β deposits could be cleared by immunotherapy by repeating the experiment using labeled 10D5 as the imaging agent at the initial imaging session. As expected, the labeled 10D5 revealed innumerable diffuse and dense-core amyloid-β deposits. The animals recovered without incident and three days later were re-imaged. Very little or no detectable fluorescence remained from the application of fluorescein-labeled 10D5 that had been administered three days before; labeled 10D5 was then re-applied directly to the cortex in both treatment groups. Repeat imaging with labeled 3D6, a monoclonal antibody that recognizes a distinct epitope on plaques (as assessed on cryostat sections), showed that few or none of the amyloid-β deposits that were present at the initial imaging remained. Amyloid angiopathy was still detected (Fig. 3). Thus, three days after a single application of anti-amyloid-β antibody, we observed dramatic resolution of amyloid-β deposits in the parenchyma. It is possible that the vascular amyloid deposits are less accessible, more stable or more rapidly replenished, as they appear largely unchanged, despite the labeling with anti-amyloid-β antibody. However, small changes in the amyloid surrounding blood vessels over three days cannot be ruled out. Replication of this experiment with 3- to 8-day delays after initial imaging in one or two sites in each of 6 animals showed nearly identical results. Sham experiments were carried out in five animals in which fluorescein-labeled antibody 16B5 was used in the initial imaging session. The initial imaging session, using antibody 16B5, did not image any amyloid-β at all. This was expected as the monoclonal antibody was not directed against an epitope present on senile plaques. Repeat imaging 3 to 5 days later using labeled 10D5 imaged numerous amyloid-β deposits that were indistinguishable from the initial imaging sessions of any of the 6 mice initially imaged with 10D5. Thus it does not appear that the surgical preparation, application of an irrelevant monoclonal antibody, or imaging *per se* led to resolution of amyloid-β deposits. As the *in vivo* immunofluorescence technique images both diffuse

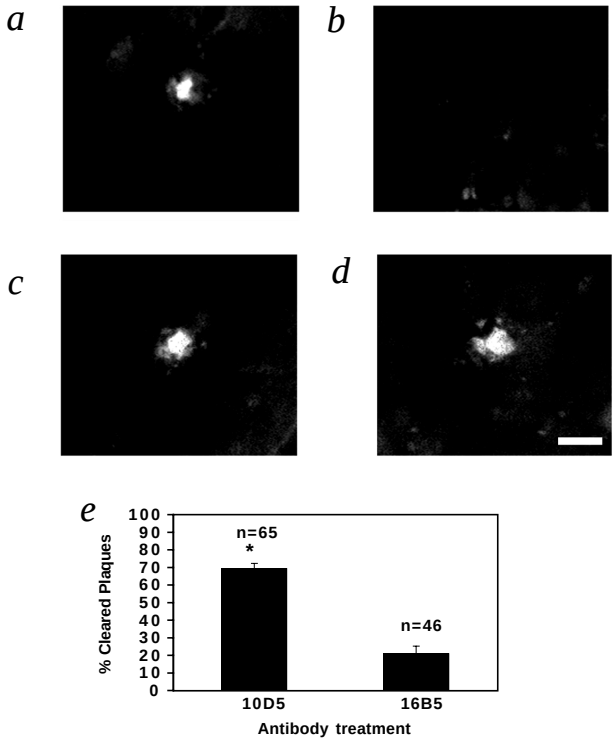

Fig. 2 Clearance of dense-core amyloid-β deposits after immunotherapy. Thioflavine S was used as the imaging agent. Anti-amyloid-β antibodies (10D5), or anti-tau antibodies (16B5), were applied to the surface of the brain at the initial imaging session for 20 min. ***a*** and ***b***, A thioflavine S-positive plaque in the first imaging session (*a*), and 3 days after application of 10D5(*b*). ***c*** and ***d***, A thioflavine S-positive plaque (*c*) in a 16B5-treated animal does not change 3 days later (*d*). Fluorescent angiography (data not shown) permitted precise alignment of the image pairs. Scale bar, 20 μm. ***e***, Quantitation of senile plaques after treatment with either 10D5 or 16B5 antibodies (*, $P < 0.001$).

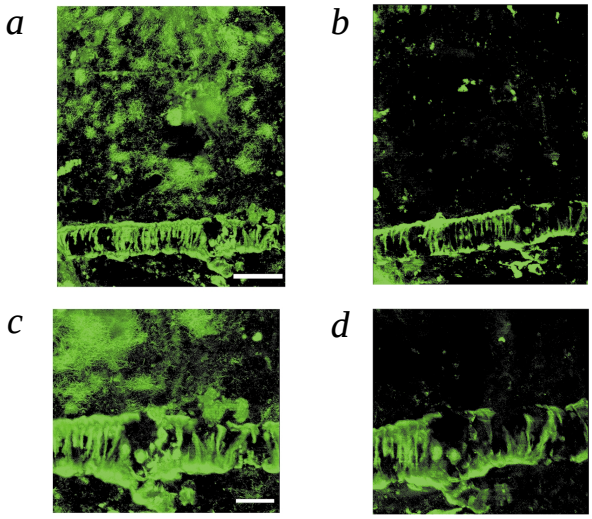

Fig. 3 *In vivo* imaging of amyloid-β deposits in 20-month-old homozygous PDAPP mice. ***a*** and ***b***, Reconstructions of stacks of Z-series images taken at 5-micron steps with a X20 objective. Initial imaging session shows numerous 10D5 immunoreactive amyloid-β plaques in the neuropil and associated with vessels in one representative animal. Scale bar, 50 μm. ***c*** and ***d***, Two-micron steps with a X60 objective starting from just below the cortical surface to approximately 150 μm below the surface taken 3 days after *a* and *b*. Amyloid-β is visualized with fluorescein-labeled monoclonal antibody 10D5. Very little of the neuropil amyloid-β remains, directly showing reversal of previously existing amyloid-β deposits. Note that the vessel-associated amyloid-β remains intact and is readily immunostained. Scale bar, 25 μm.

and dense-core amyloid-β, these results confirm and extend our observations from thioflavine-S imaging to show that both forms of amyloid-β are cleared by application of 10D5.

Histochemistry confirms reversal of amyloid-β deposits

Immunostaining with biotinylated or fluorescently tagged 3D6 showed an area, approximately 100–200 microns in depth from the surface of the skull opening, with substantially diminished amyloid-β deposits near the surface (Fig. 4) in all mice treated with 10D5, but in none of the sham-treated mice, as judged by a blinded observer. These results corroborate clearance of amyloid-β deposits after initial treatment of the cortex with direct application of 10D5.

Histochemical staining for microglia cells revealed a marked upregulation of microglia at the site of imaging (Fig. 5), even in animals treated with 16B5. At most, we observed a slight astrocyte response using immunostaining with antibody against glia fibrillary acidic protein (data not shown). These data indicate that clearance of amyloid-β after exposure to 10D5 is a specific response to anti-amyloid-β antibodies rather than a nonspecific response to injury.

Association of microglia with amyloid-β deposits

We next studied the interaction between amyloid-β and microglia at the site of antibody application because immunization with amyloid-β leads to an apparent ingestion of amyloid-β by microglia[7]. We observed a marked microglial response completely surrounding the small amounts of remaining amyloid-β at the treatment site (Fig. 6*a*). Distal to the site, typical plaques had just a few associated microglia (Fig. 6*b*). Though activation of microglia occurred in both the treated and control animals near the imaging site, the association of microglia with amyloid-β deposits was dramatically enhanced following 10D5 treatment.

Here we describe a powerful *in vivo* multiphoton imaging technology that allows visualization of distinct brain structures, in a living anesthetized mouse, with a resolution of approximately 1 μm. This provides extraordinary *in vivo* images of individual cells or pathological structures, with a resolution that far exceeds other *in vivo* technologies. In principle, any extracellular epitope could be visualized by *in vivo* immunofluorescence. The antibody penetrated as deeply as our current multiphoton microscope could detect—about 150 μm from the surface of the brain, or into layers II or III of the mouse cortex. Other fluorescent markers reveal the vascular anatomy and provide neurohistological information. Repeat imaging of the same site hours or days later can be readily obtained, and this can be extended to weeks with modifications in the protocol. This ability to chronically image the same site in a living mouse makes this experimental approach suitable for studies of diverse therapeutic interventions.

Using this novel technique, we show for the first time reversal of existing amyloid-β deposits in the brain due to an experimental intervention. We observed a remarkable clearing of thioflavine S-stained amyloid-β deposits within three days of treatment by direct application of an anti-amyloid-β antibody to the cortex. The remaining amyloid-β appears to be surrounded by microglia. Parallel studies performed in an

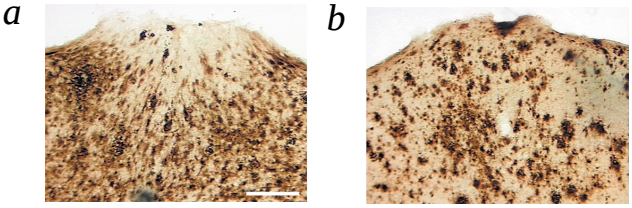

Fig. 4 Histological analysis of imaged brains from 20-month-old homozygous PDAPP mice using biotinylated antibody 3D6 shows an extraordinarily high level of amyloid-β deposits throughout the cortex and hippocampal formation. There was a marked diminution of amyloid-β staining at the site of 10D5 application. Mice brains were sectioned at 40 microns. ***a***, Immunostaining with 3D6, an anti-amyloid-β monoclonal antibody that has a distinct epitope (aa1–5), compared to 10D5 (aa3–6), showed a 100–200-micron deep area that was essentially devoid of diffuse amyloid-β deposits, in contrast to the intense deposits found in adjacent sections or medial or lateral to the site. ***b***, No changes in 3D6 immunoreactive amyloid-β plaques were observed after initial treatment with 16B5 application. Scale bar, 200 μm.

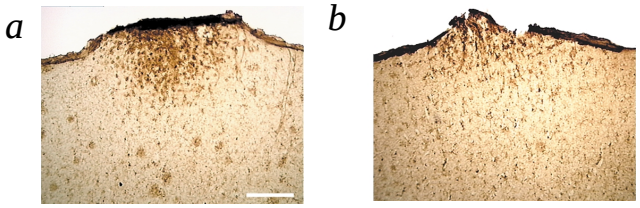

Fig. 5 Marked local microglial activation, as assessed with biotin-labeled tomato lectin, occurs 3 days after the skull preparation and imaging. ***a***, The 10D5 group. ***b***, The 16B5 group. Scale bar, 200 μm.

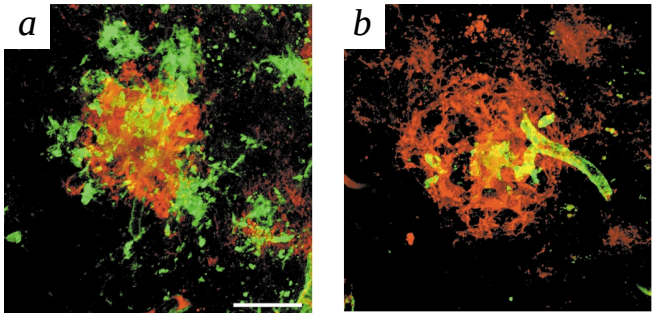

Fig. 6 Confocal thin optical sections (0.2 μm) were reconstructed to illustrate the intimate relationship of microglia with remaining amyloid-β three days after treatment with 10D5-fluorescein. Double immunofluorescence was performed with fluorescein-labeled tomato lectin and biotin-labeled 3D6 (detected with avidin-cy3 (Jackson Immunoresearch, West Grove, Pennsylvania). ***a***, Tomato lectin, which detects microglia, is shown in green, and 3D6, which detects amyloid-β, is shown in red. A marked microglial response surrounding remaining amyloid-β plaques was observed. ***b***, Distal to the site, in the temporal lobe, the association of microglia with amyloid-β is much more modest. Scale bar, 20 μm.

ex vivo system show that microglia are able to take up amyloid-β via Fc-mediated phagocytosis, which leads to subsequent peptide degradation[13]. Antibodies might also alter the fibrillogenesis of amyloid-β (ref. 14). The current experiments indicate that the humoral response mediates the attenuation of amyloid-β deposition after immunization with amyloid-β. As a result, these data support the idea that passive immunotherapy might be effective in preventing and clearing amyloid-β deposits in Alzheimer's disease. This approach, in contrast to active immunization with amyloid-β peptide, would have the clinical advantages of being self-limited, of using a reagent designed to have optimal epitope characteristics, and of avoiding the need to obtain a robust immune response in an elderly patient population.

Acknowledgments

This work was supported by grants from the National Institute on Aging (AG08487, P01AG15453 and T32GM07753), and support from the Alzheimer Association and the Walters Family Foundation. An unrestricted gift from Elan Pharmaceuticals supported housing costs for the animals.

1. Braak, H. & Braak, E. Neuropathological stageing of Alzheimer-related changes. *Acta Neuropathol.* **82**, 239–259 (1991).
2. Gomez-Isla, T. *et al.* Profound loss of layer II entorhinal cortex neurons occurs in very mild Alzheimer's disease. *J. Neurosci.* **16**, 4491–4500 (1996).
3. Davis, D.G., Schmitt, F.A., Wekstein, D.R. & Markesbery, W.R. Alzheimer neuropathologic alterations in aged cognitively normal subjects. *J. Neuropathol. Exp. Neurol.* **58**, 376–388 (1999).
4. Naslund, J. *et al.* Correlation between elevated levels of amyloid beta-peptide in the brain and cognitive decline. *JAMA* **283**, 1571–1577 (2000).

Methods

Animals were anesthetized with Avertin (Tribromoethanol, 250 mg/kg intraperitoneally). A small skull window (about 1 mm in diameter) was created using a high-speed drill (Fine Science Tools, Foster City, California). The site was moistened with artificial cerebrospinal fluid (ACSF; 125 mM NaCl; 26 mM $NaHCO_3$; 1.25 mM NaH_2PO_4; 2.5 mM KCl; 1 mM $MgCl_2$; 1 mM $CaCl_2$; 25 mM glucose) and the dura gently peeled from the surface of the brain.

The monoclonal antibody 10D5, directed against an epitope in the amino terminal half of amyloid-β (ref. 11), was labeled with fluorescein (Molecular Probes, Eugene, Oregon). Twenty minutes after adding ~1 mg/ml solution of antibody and 0.005% thioflavine S in ACSF, the solution was washed off with ACSF, the animal was placed in a head holder on a small custom-modified stage insert of an Olympus BX-50 microscope, and the site imaged using a Biorad 1024 MP microscope (BioRad, Hercules, California). The stage was equipped with X–Y encoders (Boeckler, Tuscon, Arizona), and the location of the initial imaging recorded. A fluorescent angiogram was obtained using Texas Red-labeled 70,000 MW dextran (Molecular Probes) injected into the tail vein at the time of imaging. The angiogram provides additional local landmarks to ensure that the same imaging volume is obtained at each session. Multiphoton fluorescence was generated with 750-nm excitation from a mode-locked Ti:Sapphire laser (Tsunami, Spectra Physics, Mountain View, California; 10 W Millenium pump laser). Custom-built external detectors (Hamamatsu Photonics, Bridgewater, New Jersey) collected emitted light in the range of 380–480 nm (thioflavine S), 500–540 nm (fluorescein) and 560–650 nm (Texas Red).

5. Games, D. *et al.* Alzheimer-type neuropathology in transgenic mice overexpressing V717F β-amyloid precursor protein. *Nature* **373**, 523–527 (1995).
6. Irizarry, M.C. *et al.* Abeta deposition is associated with neuropil changes, but not with overt neuronal loss in the human amyloid precursor protein V717F (PDAPP) transgenic mouse. *J. Neurosci.* **17**, 7053–7059 (1997).
7. Schenk, D. *et al.* Immunization with amyloid-beta attenuates Alzheimer-disease-like pathology in the PDAPP mouse. *Nature* **400**, 173–177 (1999).
8. Denk, W., Strickler, J.H. & Webb, W.W. Two-photon laser scanning fluorescence microscopy. *Science* **248**, 73–76 (1990).
9. Svoboda, K., Denk, W., Kleinfeld, D. & Tank, D.W. *In vivo* dendritic calcium dynamics in neocortical pyramidal neurons. *Nature* **385**, 161–165 (1997).
10. Yang, X. *et al.* Dynamic mapping at the laminar level of odor-elicited responses in rat olfactory bulb by functional MRI. *Proc. Natl. Acad. Sci. USA* **95**, 7715–7720 (1998).
11. Hyman, B.T., Tanzi, R.E., Marzloff, K., Barbour, R. & Schenk, D. Kunitz protease inhibitor-containing amyloid beta protein precursor immunoreactivity in Alzheimer's disease. *J. Neuropathol. Exp. Neurol.* **51**, 76–83 (1992).
12. Vigo-Pelfry, C. *et al.* Elevation of microtubule-associated protein tau in the cerebrospinal fluid of patients with Alzheimer's disease. *Neurology* **45**, 788–793 (1995).
13. Bard, F. *et al.* Peripherally administered antibodies against amyloid β-peptide enter the central nervous system and reduce pathology in a mouse model of Alzheimer disease. *Nature Med.* **6**, 916–919 (2000).
14. Solomon, B. *et al.* Monoclonal antibodies inhibit *in vitro* fibrillar aggregation of the Alzheimer beta-amyloid peptide. *Proc. Natl. Acad. Sci. USA* **93**, 452–455 (1996).